Title of the Grant: **Ultrasonic Nondestructive Characterization of Adhesive Bonds**

Type of Report: **Final Report**

Name of Principle Investigator: **Jianmin Qu**

Period Covered: **2/22/96 – 2/22/99**

Grantee's Institution: **Georgia Institute of Technology, Atlanta, GA 30332**

Grant Number: **NAG-1-1810**

IN-38
05-7-86

1. Introduction

Adhesives and adhesive joints are widely used in various industrial applications to reduce weight and costs, and to increase reliability. For example, advances in aerospace technology have been made possible, in part, through the use of lightweight materials and weight-saving structural designs. Joints, in particular, have been and continue to be areas in which weight can be trimmed from an airframe through the use of novel attachment techniques. In order to save weight over traditional riveted designs, to avoid the introduction of stress concentrations associated with rivet holes, and to take full advantage of advanced composite materials, engineers and designers have been specifying an ever-increasing number of adhesively bonded joints for use on airframes.

Nondestructive characterization for quality control and remaining life prediction has been a key enabling technology for the effective use of adhesive joints. Conventional linear ultrasonic techniques generally can only detect flaws (delamination, cracks, voids, etc) in the joint assembly. However, more important to structural reliability is the bond strength.

Although strength, in principle, cannot be measured nondestructively, a slight change in material nonlinearity may indicate the onset of failure. Furthermore, microstructural variations due to aging or under-curing may also cause changes in the

third order elastic constants, which are related to the ultrasonic nonlinear parameter of the polymer adhesive. It is therefore reasonable to anticipate a correlation between changes in the ultrasonic nonlinear acoustic parameter and the remaining bond strength.

It has been observed that higher harmonics of the fundamental frequency are generated when an ultrasonic wave passes through a nonlinear material. It seems that such nonlinearity can be effectively used to characterize bond strength. Several theories have been developed to model this nonlinear effect (Nagy and Adler, 1991; Achenbach and Parikh, 1991; Parikh and Achenbach, 1992; Hirose and Kitahara, 1992; and Anastasi and Roberts, 1992). Based on a microscopic description of the nonlinear interface binding force, a quantitative method was presented by Pangraz and Arnold (1994). Recently, Tang, Cheng and Achenbach (1997) presented a comparison between the experimental and simulated results based on a similar theoretical model. A through-transmission setup for water immersion mode-converted shear waves was used by Berndt and Green (1998) to analyze the ultrasonic nonlinear parameter of an adhesive bond. In addition, ultrasonic guided waves have been used to analyze adhesive or diffusion bonded joints (Lowe and Cawley, 1994, Rose, Rajana and Hansch, 1995, and Rose, Zhu and Zaidi, 1998).

In this paper, the ultrasonic nonlinear parameter is used to characterize the curing state of a polymer/aluminum adhesive joint. Ultrasonic through-transmission tests were conducted on samples cured under various conditions. The magnitude of the second order harmonic was measured and the corresponding ultrasonic nonlinear parameter was evaluated. A fairly good correlation between the curing condition and the nonlinear

parameter is observed. The results show that the nonlinear parameter might be used as a good indicator of the cure state for adhesive joints.

The report is arranged as follows. In section 2, a brief introduction is given to show how the higher order harmonics are generated by material nonlinearity. Both analytical and numerical examples are presented based on the asymptotic expansion method and the finite element method, respectively. Section 3 describes the sample and the test method. The results are presented and discussed in Section 4.

2. Generation of Higher Order Harmonics

It is well known that non-linearity, either geometrical (Bland, 1969; Richardson, 1979) or material (Kolsky, 1963), in an acoustic medium can generate higher order harmonics. For example, consider a one-dimensional problem of wave propagation through a nonlinear medium. For small strain deformation, the equation of motion can be written as

$$\frac{1}{\rho}\frac{\partial \sigma}{\partial x} = \frac{\partial^2 u}{\partial t^2} \quad , \tag{2.1}$$

where u is the displacement in the x-direction, ρ is the mass density and $\sigma(x,t)$ is the normal stress in the x-direction. For the small strain deformation considered here, the normal strain in the x-direction, $\varepsilon(x,t)$, is defined as

$$\varepsilon = \frac{\partial u}{\partial x} \quad . \tag{2.2}$$

Next, assume that the nonlinear constitutive relationship of the medium is described by

$$\sigma = Ef(\varepsilon) \quad , \tag{2.3}$$

where E can be viewed as the "elastic Young's modulus."

Substitution of (2.3) into (2.1) yields

$$\frac{1}{c^2}\frac{\partial^2 u}{\partial t^2} - \frac{\partial^2 u}{\partial x^2} = [f'(\varepsilon) - 1]\frac{\partial^2 u}{\partial x^2} \quad , \tag{2.4}$$

where $c = \sqrt{E/\rho}$ can be considered as the "phase velocity." This nonlinear equation can be solved either numerically or asymptotically once $f(\varepsilon)$ is known. To illustrate the solution characteristics, let us expand $f(\varepsilon)$ into power series of ε and take only the first two terms in the expansion so that

$$f(\varepsilon) = \varepsilon(1 - 0.5\gamma\varepsilon) \quad , \tag{2.5}$$

where γ is a parameter that indicates the amount of material non-linearity. Obviously, for linear elastic materials, $\gamma = 0$. Fig. 2.1 shows several stress-strain curves for $\gamma = 0$, 1.0,10, and 30, respectively. Note that the constitutive equation given by (2.5) dictates that the material behaves differently in tension and compression, although the difference is only to the second order. In the literature, such material behavior is sometimes referred to as pseudo elastic. To describe the complete symmetry in tension and compression, one should retain only the terms with odd exponents of ε. Since the primary objective here is to illustrate the possibility of generating second order harmonics, only the term with ε^2 is used here for algebraic simplicity.

Now, consider a layer of nonlinear material with layer thickness h. The material follows the constitutive law given in (2.5). A plane wave $A\sin(kx - \omega t)$ is prescribed on the left side of the layer, i.e.,

$$u(0,t) = A\sin(\omega t) \quad , \tag{2.6}$$

where k is the wavenumber and ω is the circular frequency. The displacement on the right hand side of the layer can then be obtained from (2.4) – (2.6) through a simple asymptotic analysis (Truell, et al., 1969),

$$u(h,t) \approx A_1 \sin(kh - \omega t) + A_2 \cos(2kh - 2\omega t) \quad , \tag{2.7}$$

where

$$A_2 = \frac{\gamma}{8} k^2 h A_1^2 = \frac{\gamma}{8c^2} \omega^2 h A_1^2 \quad . \tag{2.8}$$

It is clear from the above solution that the material nonlinearity distorts the waveform and generates the second order harmonic. In other words, after propagating through a nonlinear medium, a single frequency wave may contain frequency components other than the fundamental frequency. Usually, the amplitudes of the higher order harmonics are much less than the amplitude of the fundamental component. In the reminder of this paper, the amplitude of the fundamental component is simply referred to as the wave amplitude to avoid ambiguity unless otherwise indicated.

It is interesting to note the relationship between γ and the ultrasonic nonlinear parameter defined by Yost and Cantrell [Cantrell and Yost, 1990; Yost and Cantrell, 1990],

$$\beta = \frac{8A_2}{k^2 h A_1^2} = \gamma \, . \tag{2.9}$$

By definition, γ is an intrinsic material property representing the amount of nonlinearity in the stress-strain relationship. However, because of the asymptotic nature of solution (2.7), the second equal sign in (2.9) only holds for very small values of γ. Thus, strictly speaking, β becomes material constant only when the material nonlinearity is small or when the amplitude of the incident waves is small [Yost and Cantrell, 1990]. For higher values of γ, the ultrasonic nonlinear parameter β becomes dependent not only on the material, but also on the incident wave. Such dependency, in principle, can be found by

continuing the asymptotic analysis to higher order terms. However, the algebra becomes rather complex.

To observe higher order terms more easily, a finite element analysis of the adhesive joint was conducted. The one-dimensional numerical model is shown in Fig. 2.2. A 5-cycle harmonic load of 2MHz was applied as the incident wave. The thickness of the adhesive layer is 0.24mm. At 2 MHz, the wavelength in the adhesive is about 3.3 mm. In the numerical calculations, the stress-strain relationship given by (2.5) was used with $\gamma = 0$, 1.0,10, and 30, respectively. The computation was carried out using the finite element program ABAQUS, and stress field was obtained as a function of time. For $\gamma = 10$, Fig. 2.3 shows the Fourier transform of the stresses at three locations, A, B and C, as indicated in Fig. 2.2. Note that, at point A, the wave has not reached the nonlinear region yet and therefore, can be viewed as the incident wave. Point B is at the center of the adhesive, while point C is at a location after the wave has gone through the adhesive.

Fig. 2.3 clearly shows that the higher order harmonics are indeed generated by the nonlinearity of the adhesive material. Higher order harmonics can be seen clearly up to the third order (the peak at 6 MHz) for the case considered here.

Comparison of the corresponding nonlinear parameter β is given in Fig. 2.4 for different values of γ. It is seen clearly from Fig. 2.4 that higher value of γ yields higher nonlinear parameter β. However, the relationship between β and γ is not linear. This indicates that the asymptotic solution (2.7) has a very limited range of applicability.

3. Through Transmission Measurements

Through transmission tests were conducted, in order to measure the higher order harmonics and to correlate the amplitude of the higher order harmonics to the cure state

of the adhesive joints. This section discusses sample preparation, test setup and the measurement methods used in the through transmission tests.

Test Samples

The test samples used in this study were provided by the Boeing Co. The samples consist of two aluminum plates bonded together by an adhesive layer. The adhesive is a thermosetting modified epoxy, AF-163-2K, in sheet form (knit supporting carrier) made by the 3M Company. The plates are 2024 aluminum. Relevant material constants are listed in Table 1.

As illustrated in Fig. 3.1, the bonded area of the specimen is 12.7 cm x 17.8 cm (5.0" x 7.0"). The adhesive (bondline) thickness is approximately 0.32 mm (12.6 mils) and the adherend's thickness is 1.6 mm (63 mils).

The aluminum plates were anodized and primed prior to application of the adhesive. The joint was then placed in a temperature/pressure oven for curing. All four samples used in this study were prepared with the same procedure except the curing conditions. The different curing schedules for the four samples are listed in Table 2.

The resulting bond strengths due to different curing schedules are also listed in Table 2. The normal (optimal) curing schedule is 121°C (250°F) for 90 minutes under 0.34MPa (50 psi). Sample A was cured under this condition. It is seen that samples with different state of curing show drastically different bond strength. It is anticipated that such differences in the curing state can be characterized nondestructively and correlated with the higher order harmonics.

Experimental Setup

A block diagram of the experimental set up is shown in Fig 3.2. A 40 cycle time-harmonic signal of 2MHz was generated by a Wavetek function generator. The signal was amplified by a high voltage amplifier (ENI, DC ~ 10MHz, 50dB) to obtain a high amplitude driving voltage for the generating transducer. A typical output signal of the function generator and the amplifier are shown in Fig. 3.3. The highest output voltage of the amplifier used in the experiment was 350 volts. A narrow-band contact PZT transducer was used as the generating transducer. Its center frequency is 2MHz (Ultran, KC50-2, 1.25MHz at -6dB). The incident ultrasonic wave from the generating transducer was transmitted perpendicularly through the adhesive layer. The receiver is a narrow-band contact PZT transducer with 4MHz center frequency (Ultran, KC50-4, 3.5MHz at -6dB). The output signal $f(t)$ of the receiver was recorded by an oscilloscope (Tektronix, 150MHz) and analyzed on a personal computer. A typical received signal is shown in Fig. 3.4.

The sample and the two contact PZT transducers were fixed by two aluminum plates with a cylindrical cavity on each side, respectively, to hold the transducers at the same position as shown in Fig. 3.5. For efficient signal generation, a coupling liquid was used between the transducer and the sample. In addition, pressure on the transducer/sample interface can be varied by adjusting the four screws on the fixture.

Testing and Signal Processing

During the through transmission test, a 40-cycle time-harmonic signal of 2MHz was generated by the function generator, then amplified by the high voltage amplifier and sent to the generating transducer. The signal received by the receiving transducer, $f(t)$,

was recorded by the oscilloscope. Finally, the data was processed using the Fast Fourier Transform (FFT) to obtain the frequency spectra,

$$F\left(\frac{m}{N\Delta t}\right)=\frac{1}{N}\sum_{n=0}^{N-1} f(m\Delta t)\exp(2\pi imn/N),\ m=0,1,2\ \ldots\ \ldots\ N\text{-}1 \qquad (3.1)$$

where N is the total number of sampling points and Δt is the time interval between the sampling points.

The amplitude of the fundamental frequency and the higher order harmonic components can then be defined as (see Appendix)

$$A_n=\left|F\left(\frac{n\omega_0}{2\pi}\right)\right|,\qquad n=1,2,3\ldots \qquad (3.2)$$

where ω_0 is the fundamental circular frequency of the generating transducer. In this study, $f_0=\omega_0/2\pi=2\text{MHz}$ was used.

The amplitude of the fundamental frequency component, A_1, in the received signal $f(t)$ is plotted in Fig. 3.6 as a function of the incident voltage V_i. The linear relationship between A_1 and V_i confirms that the generation and receiving systems are operating in their linear regime within the voltage range used.

Following (2.9), the nonlinear parameter of the adhesive is thus defined by

$$\beta=\frac{8A_2}{k^2hA_1^2}\ . \qquad (3.3)$$

This nonlinear parameter will be used to characterize the cure state of the adhesive joints.

Since β depends on the amplitude of the incident wave, care must be given to ensure that the same incident wave is used for all samples, if one needs to compare the β values between different samples. To this end, the tightness of the transducer/sample

assembly in each test is adjusted through the adjustable screws in the test apparatus so that the received signals have the same amplitude for all the samples.

4. Results and Observations

Values of the nonlinear parameter β were measured using the procedures described in the previous sections. The results obtained from the three samples cured under various curing schedules (detailed in Table 2) were obtained and are presented in Fig. 4.1. Note that sample B1 was cured under the optimal conditions, while samples B2 and B3 were under-cured (lower temperature and shorter time). Clearly, the under-cured samples show higher values of the ultrasonic nonlinearity parameter. The more under cured the sample is, the higher the nonlinear parameter β.

As a final remark, it should be mentioned that the analytical and numerical analyses of Section 2 indeed indicate that higher order harmonics are generated by the material nonlinearity, and the experimental tests collaborate this, showing a significant increase in the nonlinear parameter for under-cured adhesives. However, the fundamental relationship between the curing state and the amount of nonlinearity in the adhesive is still an open question; This study only demonstrates that there is indeed a correlation between the nonlinear parameter and the curing state. Further investigation is needed to establish the quantitative relationship between the nonlinear parameter and the degree of curing.

References

J. D. Achenbach and O. K. Parikh, "Ultrasonic analysis of nonlinear response and strength of adhesive bonds," J. Adhesion Sci. Technol. Vol. 5, No. 8, pp. 601-618 (1991).

R. F. Anastasi and M. J. Roberts, "Acoustic Wave propagation in an adhesive bond model with degrading interfacial layers," MTL TR 92-63, U.S. ARMY Materials Technology Laboratory (1992).

T. P. Berndt and R. E. Green, "Feasibility study of a nonlinear ultrasonic technique to evaluate adhesive bonds," Private communication (1998).

D. R. Bland, Nonlinear Dynamic Elasticity, Blaisdell Publishing Company, Waltham, Massachusetts (1969).

A. Bostrom and G. Wickham, "On the boundary conditions for ultrasonic transmission by partially closed cracks," J. of NDE, Vol. 10, pp.139-199, (1991).

J. H. Cantrell and W. T. Yost, "Material Characterization using acoustic nonlinearity parameters and harmonic generation: Effects of crystalline and amorphous structures," Review of Progress in QNDE, Vol. 13B, pp. 1661-1668 (1990).

S. Hirose and M. Kitahara, "Time domian BIE applied to flaw type recognition," Review of Progress in QNDE, Vol. 10A, pp.75-82 (1992).

H. Kolsky, Stress Waves in Solids, Dover Publications, New York (1963).

G. M. Light and H. Kwun, "Nondestructive evaluation of adhesive bond quality, State-of-the-art review," NTIAC-89-1, June 1989.

M. J. S. Lowe and P. Cawley, "The applicability of plate wave techniques for the inspection of adhesive and diffusion bonded joints," J. of NDE, Vol. 13, pp. 185-199 (1994).

P. B. Nagy, P. McGowan, and L. Adler, "Acoustic nonlinearities in adhesive joints," Review of Progress in QNDE, Vol. 9, pp. 1685 - 1692 (1991).

S. Pangraz and W. Arnold, "Quantitative determination of nonlinear binding forces byultrasonic technique," Review of Progress in QNDE, Vol. 13B, pp. 1995-2001 (1994).

O. K. Parikh and J. D. Achenbach, " Analysis of nonlinearly viscoelastic behavior of adhesive bonds," J. of NDE, Vol. 11, pp. 221-226 (1992).

J. M. Richardson, "Harmonic generation at an unbounded interface - I. Planar interface between semi-infinite elastic media," Int. J. of Engineering Science, Vol. 17, pp. 73-85 (1979).

J. L. Rose, K. M. Rajana and M. K. T. Hansch,"Ultrasonic guided waves for NDE of adhesively bonded structures," J. of Adhesion, Vol. 50, pp. 71-82 (1995).

J. L. Rose, W. Zhu and M. Zaidi, "Ultrasonic NDT of titanium diffusion bonding with guided waves," Materials Evaluation, Vol. 56, No. 4, pp. 535-539 (1998).

Z. Tang, A. Cheng and J. D. Achenbach, "An ultrasonic technique to detect nonlinear behavior related to degradation of adhesive bonds," Review of Progress in QNDE, 1997 (in press).

R. Truell, C. Elbaum and B.B. Chick, "Ultrasonic Methods in Solid State Physics," Academic Press, New York, (1969).

W. T. Yost and J. H. Cantrell, "Material Characterization using Acoustic Nonlinearity Parameters and Harmonic Generation: Engineering Materials," Review of Progress in QNDE, Vol. 13B, pp. 1669-1676 (1990).

Appendix

First, consider a time domain signal

$$f(t) = A_n \exp(-in\omega t) \tag{A.1}$$

Substitution of (A.1) into (3.2) yields

$$F\left(\frac{m}{N\Delta t}\right) = \frac{A_n}{N}\sum_{k=0}^{N-1}\exp\left[2\pi i(m - \frac{n\omega N\Delta t}{2\pi})\frac{k}{N}\right]. \tag{A.2}$$

Next, by making use of the identity

$$\lim_{N\to\infty}\frac{1}{N}\sum_{k=0}^{N-1}\exp\left[2\pi i(m-n)\frac{k}{N}\right] = \delta_{mn} \tag{A.3}$$

in (A.2), one concludes that

$$F\left(\frac{m}{N\Delta t}\right) = \begin{cases} 0 & \text{when } \dfrac{m}{N\Delta t} = \dfrac{n\omega}{2\pi} \\ A_n & \text{when } \dfrac{m}{N\Delta t} = \dfrac{n\omega}{2\pi} \end{cases} \tag{A.4}$$

or,

$$F\left(\frac{n\omega}{2\pi}\right) = A_n \quad . \tag{A.5}$$

This proves (3.2).

Table 1 Material properties of Al2024 and AF-163-2K

	ρ(kg/cm^3)	E(GPa)	ν
Al2024	2.78	73.0	0.35
AF-163-2K	1.21	1.1	0.34

Table 2 Curing conditions and the bond strength (obtained through destructive tests) for the different samples

Sample Number	B1	B2	B3
Curing Temp. (°C)	121	90	82
Curing Time (min.)	90	60	60
Bond Strength (MPa)	35	4.1	4.0

Figure Captions:

Fig. 2.1 Stress-strain curves for $\gamma = 0$, 1.0,10, and 30, respectively.

Fig. 2.2 Schematic of the adhesive joint.

Fig. 2.3 Finite element prediction of higher order harmonics.

Fig. 2.4 Finite element prediction of the nonlinear parameter as a function of γ.

Fig. 3.1 Sample geometry

Fig. 3.2 Experimental setup.

Fig. 3.3 Input signal (after the amplifier).

Fig. 3.4 Signal (after passing through the joint) recorded by the oscilloscope.

Fig. 3.5 Sample holder.

Fig. 3.6 Relationship between A_1 and A_2.

Fig. 4.1 The nonlinear parameter for the different samples.

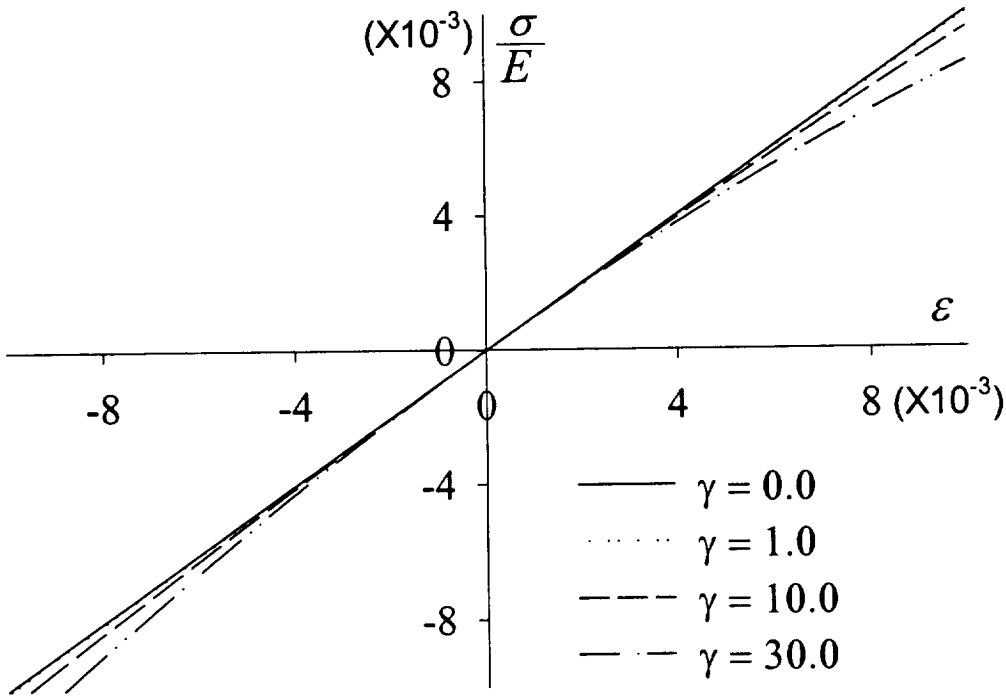

Fig. 2.1 Stress-strain curves for $\gamma = 0$, 1.0,10, and 30, respectively.

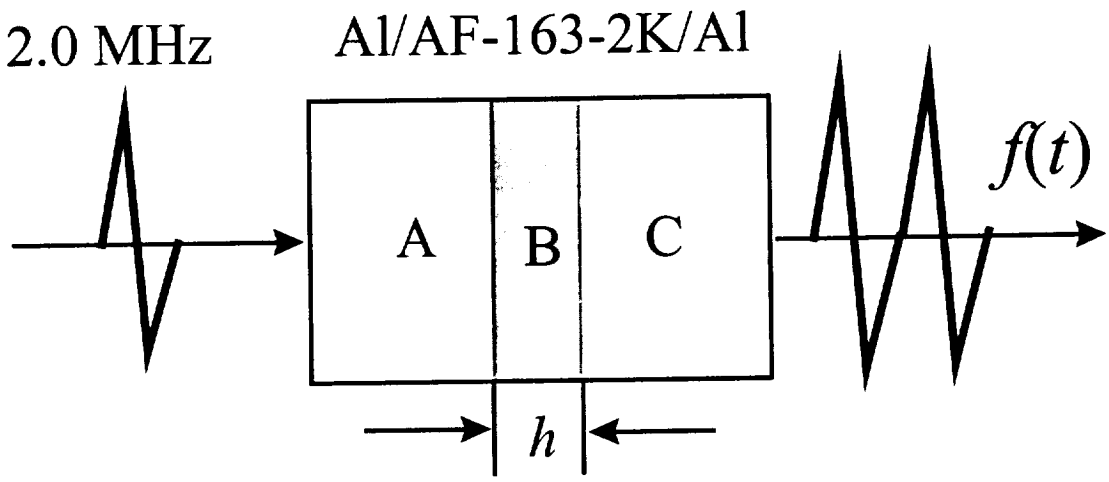

Fig. 2.2 Schematic of the adhesive joint.

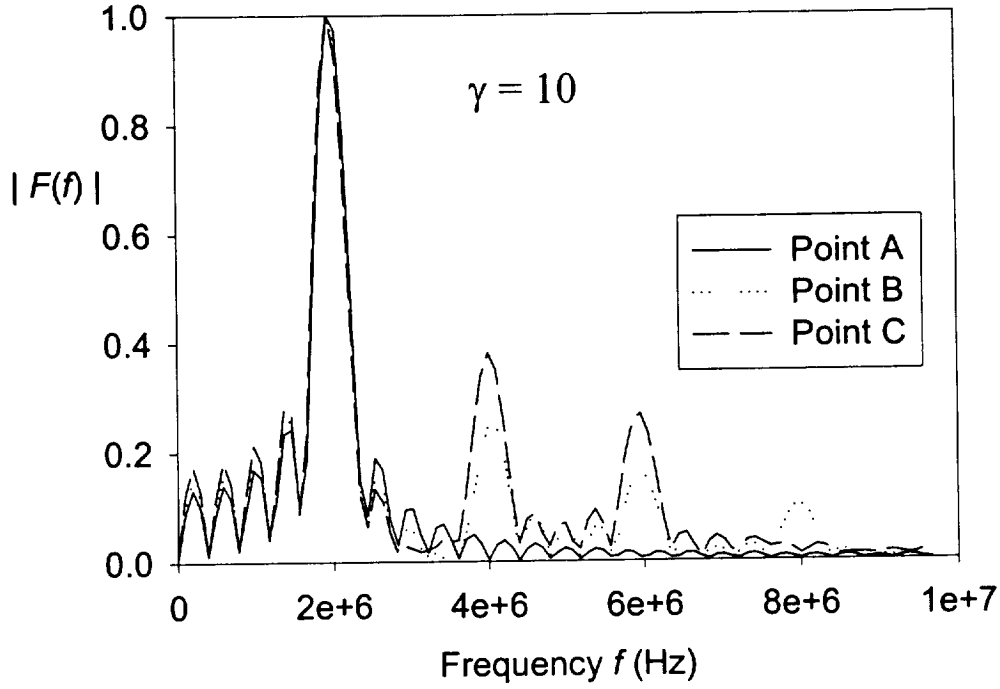

Fig. 2.3 Finite element prediction of higher order harmonics.

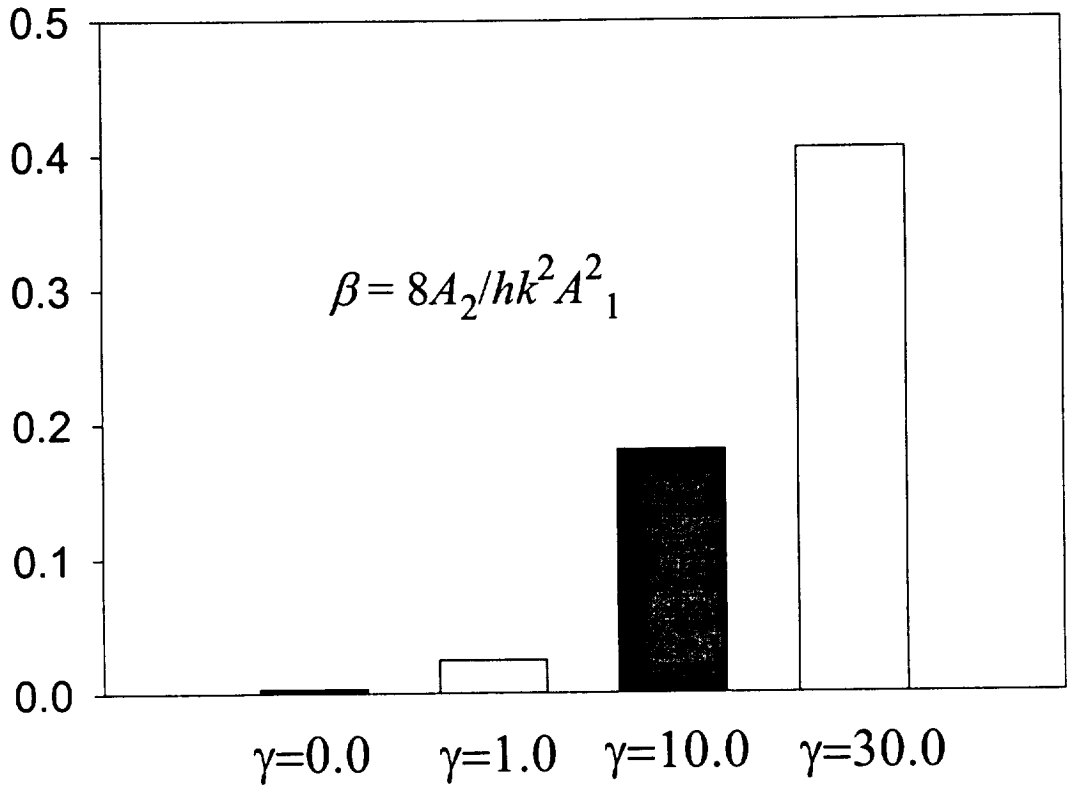

Fig. 2.4 Finite element prediction of the nonlinear parameter as a function of γ.

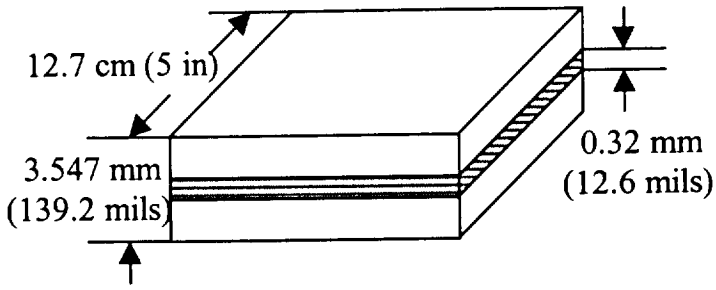

Fig. 3.1 Sample geometry

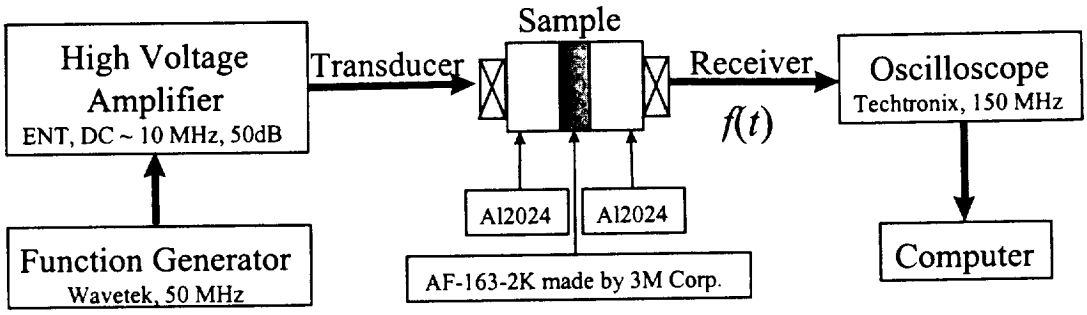

Fig. 3.2 Experimental setup.

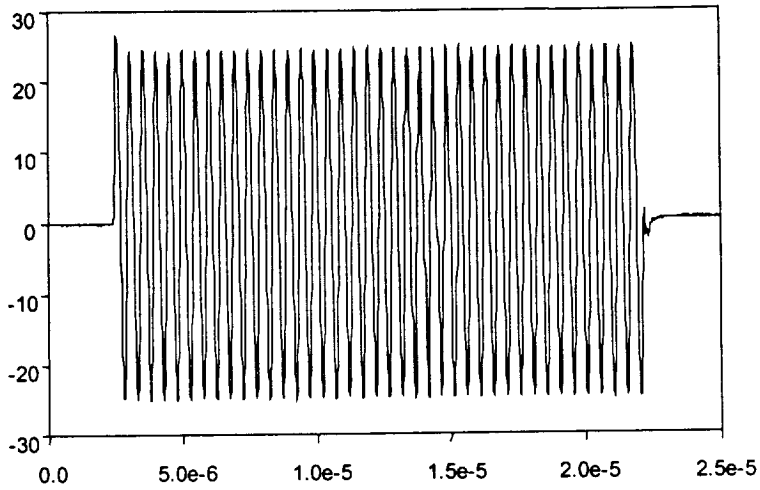

Fig. 3.3 Input signal (after the amplifier).

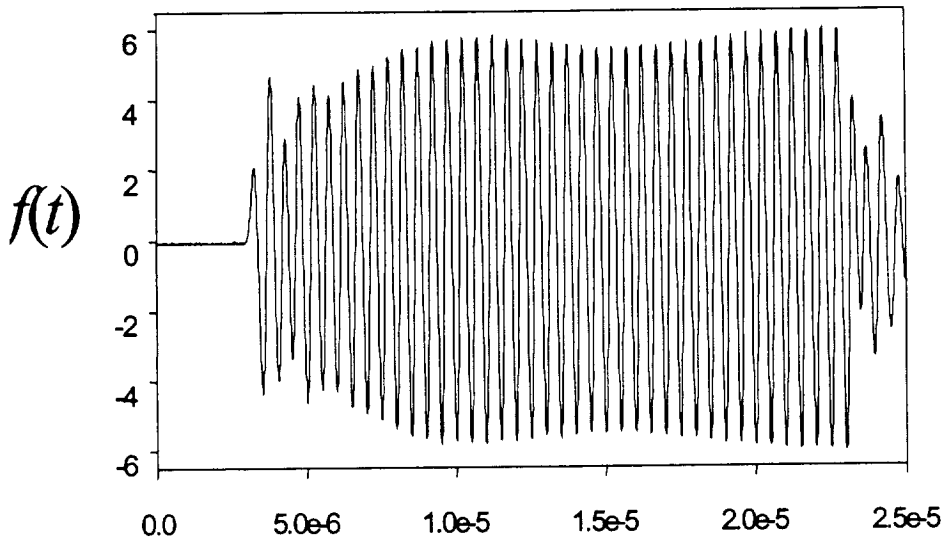

Fig. 3.4 Signal (after passing through the joint) recorded by the oscilloscope.

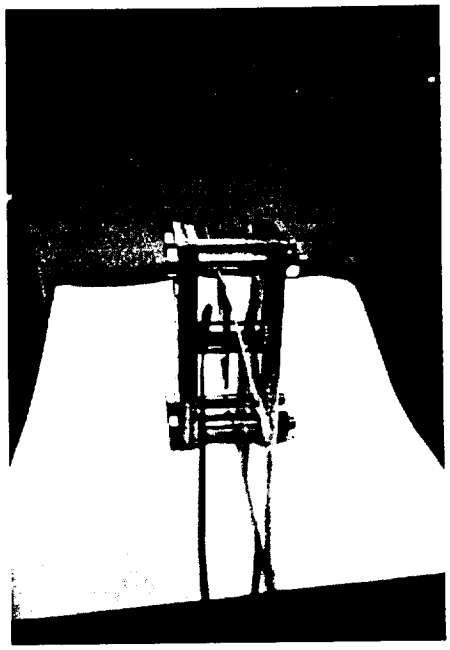

Fig. 3.5 Sample holder.

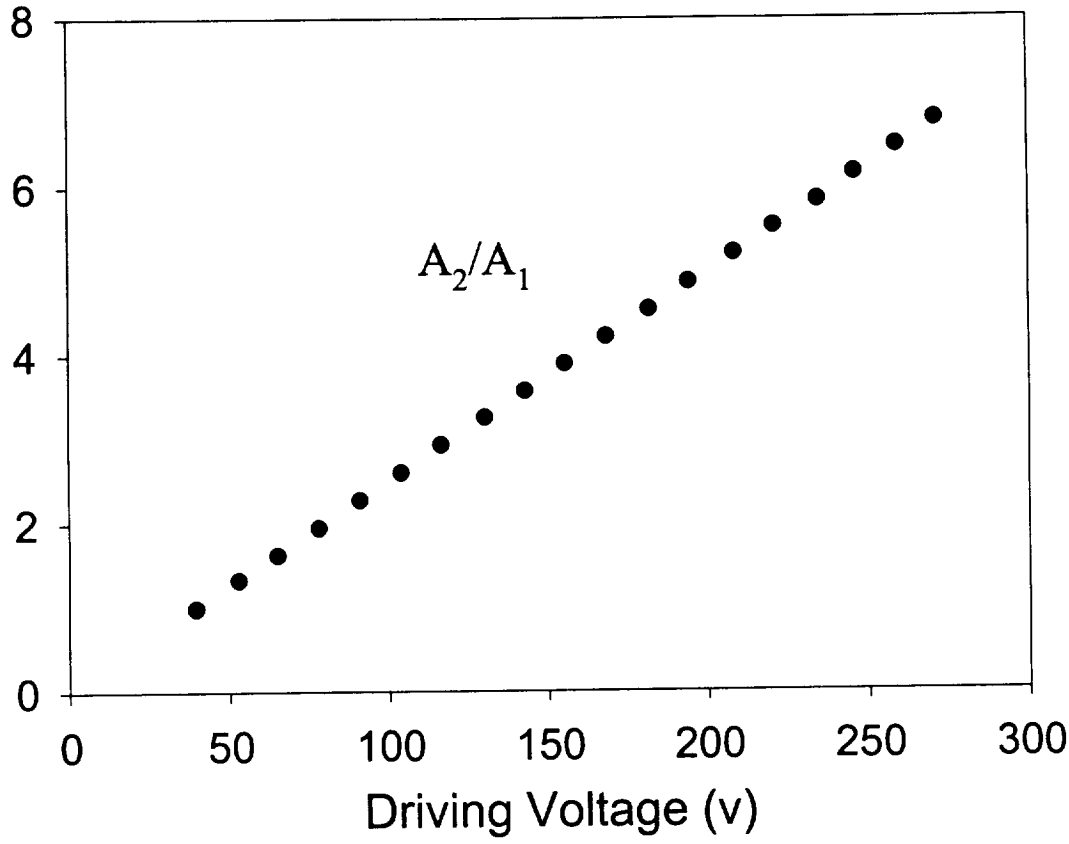

Fig. 3.6 Relationship between A_1 and A_2.

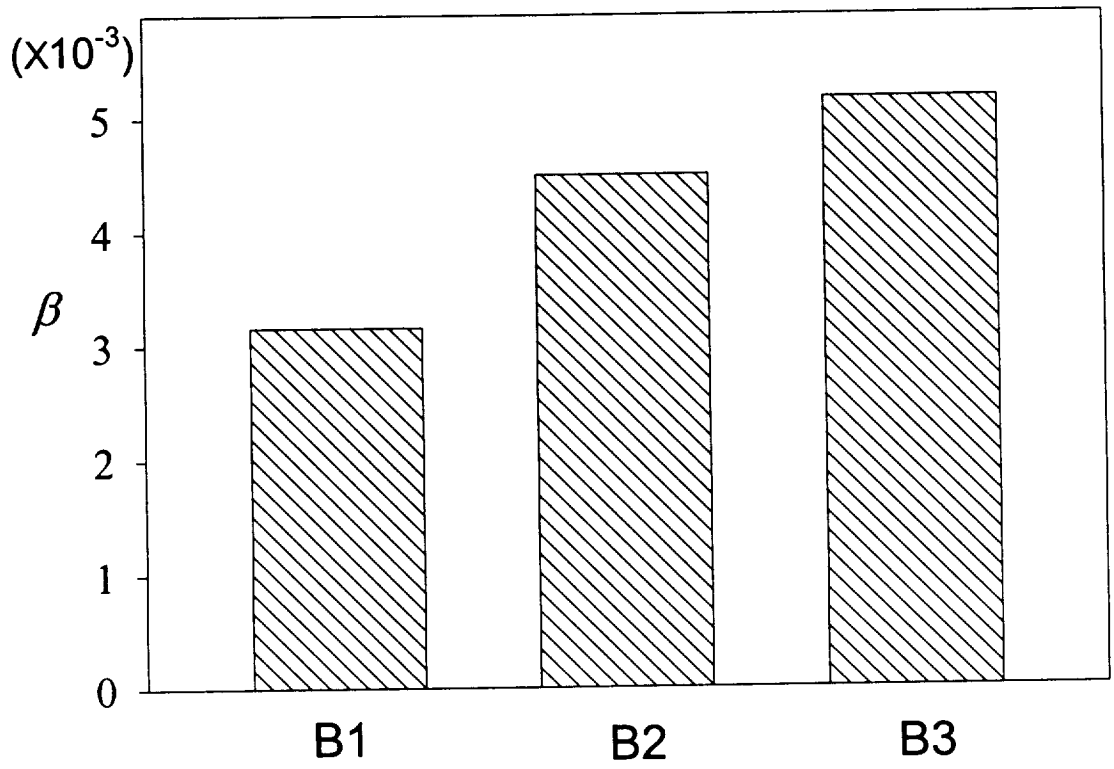

Fig. 4.1 The nonlinear parameter for the different samples.